Water Vapor Measurement and Compensation in the Near- and Mid-Infrared with the Keck Interferometer Nuller

Chris Koresko[a] M. Mark Colavita[b] Eugene Serabyn[b] Andrew Booth[b] and Jean Garcia[b]

[a]Michelson Science Center, IPAC, Caltech, Pasadena, CA 91125, USA;
[b]Jet Propulsion Laboratory, Caltech, Pasadena, CA 91109, USA

ABSTRACT

Water vapor is the dominant source of randomly-changing atmospheric dispersion on timescales of seconds to minutes in the near- and mid-infrared. The dispersion changes are sufficient to limit the performance of the Keck Nuller unless steps are taken to measure and compensate for them. Here we present the first measurements of water vapor differential column fluctuations with the mid-infrared Keck Nuller and its near-infrared fringe tracker, taken in October 2005, and discuss theoretical and practical aspects of our dispersion feedforward implementation. The data show much larger fluctuations than were seen in median Mauna Kea conditions measured at radio wavelengths, and probably account for the generally poor performance of the Nuller during the observing run. The measurements in the two bands show strong correlations, indicating that the planned feedforward of the near-infrared value to stabilize the dispersion in the mid-infrared will substantially reduce the residual dispersion fluctuations seen by the Nuller.

Keywords: Interferometry, Nulling, Water Vapor, Feedforward

1. INTRODUCTION

Nulling interferometry is a high-contrast detection technique which relies on the suppression of on-axis starlight by a central destructive interferometric fringe, or "null". The goal is to reduce the contribution from the star by a large enough factor make much fainter, off-axis astrophysical flux, e.g., due to an extended disk or a faint companion star, detectable. In the case of a single-baseline, pupil-plane beam combiner such as the Keck Interferometer Nuller (KIN), no image is formed and the detection is made photometrically by comparing the measured fraction of the total light which leaks through the null to the prediction which is typically derived from a model in which the star is a disk of known angular diameter and surface brightness.[1]

In practice, the leakage through the null can be approximated as the sum of several instrumental terms terms, collectively called the *system leakage*, and the *astrophysical leakage* which is the integral over the sky of the product of the true image of the astrophysical source and the response pattern of the interferometer (the "beam"). The system leakage can be regarded as the sum of terms which are determinable from the observations of the science target itself, and which are likely to fluctuate significantly over timescales shorter than the measurement time (typically a few minutes to a few hours) plus terms which cannot readily be measured without reference to a separate calibration target. The latter terms are necessarily assumed to vary slowly compared to the time between science target and calibration target observations.

Longitudinal dispersion, i.e., the wavelength dependence of the null fringe position, is one of the more important instrumental leakage sources in the former category. The Nuller design includes dispersion controllers which can be thought of as plane parallel ZnSe plates of adjustable thickness.[2] These are normally adjusted to produce an approximately achromatic wavefront across the Nuller's bandpass before observing begins, and fine-tuned by a servo control system during observations to track dispersion changes.

In the limit of large SNR, one could measure the fringe phase as a function of wavelength across KIN's effective bandpass and use that information directly to derive optimal settings for the delay lines and dispersion controllers. This is generally not possible in practice because both the band-averaged fringe phase and the dispersion fluctuate more rapidly than they can be derived from mid-infrared measurements of stars as faint

Send correspondence to C. Koresko at koresko@ipac.caltech.edu or (818) 354 6680

as typical KIN targets. While the fluctuations in the band-averaged phase are due primarily to temperature fluctuations in the "dry-air" components of the atmosphere, i.e., everything other than water, the dispersion fluctuations are produced mainly by the changing columns of water. Water is highly dispersive in the infrared and is typically not well-mixed in the atmosphere.

The solution is to use the near-infrared K-band measurements on the same long baselines to measure the differential column density of water vapor on short timescales, while simultaneously measuring them on longer timescales in the mid-infrared. The photometric SNR of the K-band data is generally much higher than that in the mid-infrared. This is because of the combination of a much lower thermal infrared background and the availability of near-infrared detector arrays with lower readnoise. The information from the K band is fed forward to the mid-infrared delay lines and dispersion controllers to filter out the rapid fluctuations, leaving only the slower changes which can be adequately derived from the mid-infrared data after passing them through a long filter.

Successful application of this technique requires accurate knowledge of the refractivity of water and an understanding of the (rather simple, but nontrivial to measure) underlying physics. Here we describe the method used to predict the phase and group delays in the Nuller bandpass from K-band fringe tracker data, and report the results of early tests with KIN on the sky, taken in October 2005. The tests confirm that the phase and dispersion of the mid-infrared fringes can be predicted from their values in the K band. However, there remain some puzzling aspects of these data.

2. UNDERLYING PHYSICS

The refractivity of water vapor in the infrared is a complicated function of wavelength because water exhibits strong absorption resonances between and within the infrared passbands. (In fact, the water absorptions are largely responsible for defining these passbands.) We rely on a computation of the refractivity as a sum over the contributions from the various UV and infrared resonances[3] as tabulated in the HITRAN96 database.[4]

The interferometer servo system computes and reacts only to the broadband fringe phase and to the linear part of its wavelength dependence (the *group delay*). From this point of view, water produces two important dispersion effects, which we refer to as *interband* and *intraband* dispersion.

2.1. Interband Dispersion

The inter-band dispersion is the result of the difference in the refractivity averaged across the near-infrared K band relative to its average across the mid-infrared Nuller bandpass. Its effect is to cause the mean position of the null fringe to drift with respect to the K-band fringe as the differential water column changes. This is important since the K-band fringe tracker is the primary source of information about the position of the mid-infrared fringe on short timescales; naively setting the Nuller's delay lines to follow the K-band fringe would leave significant fringe motions uncorrected.

As a concrete example, the refractivity of a molecule of water vapor at 2.2 μm (the center of the near-infrared K band) is $N^w_{2.2} = 9.0\times 10^{-24}$ cm^3 but at 10.5 μm in the Nuller's bandpass it is only $N^w_{10.5} = 6.5\times 10^{-24}$ cm^3. The refractivity of an average "dry-air" molecule is $N^d = 1.1 \times 10^{-23}$ cm^3 at both wavelengths. In median conditions at Mauna Kea, the differential water column density fluctuations for a 100 m baseline are $\sigma^{15}_\Sigma = 3.7 \times 10^{19}$ cm^{-2} RMS over a 15-minute period.[5] Under the usual assumption of constant pressure, each water molecule merely substitutes for a dry-air molecule, and the change in the fringe position depends the difference in their refractivities. The resulting RMS fringe position changes due to water-vapor seeing are

$$\begin{aligned} \sigma_{2.2} &= \sigma^{15}_\Sigma(N^w_{2.2} - N^d) = -0.6\ \mu\text{m} \\ \sigma_{10.5} &= \sigma^{15}_\Sigma(N^w_{10.5} - N^d) = -1.5\ \mu\text{m} \end{aligned} \quad (1)$$

The corresponding RMS of the difference between the 2.2 μm and 10.5 μm fringe positions is

$$\sigma_{interband} = \sigma^{15}_\Sigma(N^w_{2.2} - N^w_{10.5}) \quad (2)$$

which is 0.9 μm. This gives an indication of the broadband OPD error that would result from ignoring the water vapor seeing and relying solely on the K-band fringe position to stabilize the mid-infrared fringe.

2.2. Intraband Dispersion

The effect of the intraband dispersion is somewhat more complex because the wavelength dependence of the refractivity of water is significantly nonlinear across the Nuller bandpass. To first order, however, it can be regarded as simply adding a group delay to the mid-infrared fringe. The size of this effect can be calculated straightforwardly from the refractivity of water at a few representative wavelengths and the amplitude of the differential column density fluctuations. For the purpose of this presentation we choose wavelengths of 8.5 and 12.5 μm to roughly span the Nuller bandpass, and 2.0 and 2.4 μm to span the K band. The refractivity of water for these wavelengths is given in Table 1.

Within the Nuller bandpass the RMS relative OPD offset produced by water vapor is easily found by analogy with Equation (2):

$$\begin{aligned} \sigma_K = &\quad \sigma_\Sigma^{15}(N^w_{2.0} - N^w_{2.4}) = &\quad 0.06\ \mu\text{m} \\ \sigma_{nuller} = &\quad \sigma_\Sigma^{15}(N^w_{8.5} - N^w_{12.5}) = &\quad 1.0\ \mu\text{m} \end{aligned} \tag{3}$$

We see that the phase difference due to water is a factor of around 16 larger across the Nuller bandpass than it is across the K band, and that the intraband dispersion in the Nuller bandpass is comparable to the K-vs-Nuller interband dispersion.

2.3. Dispersion Metric

The fringe phase ϕ at OPD x can be written as

$$\phi = kx + k\Sigma N^w \tag{4}$$

where $k = \frac{2\pi}{\lambda}$ is the wavenumber and Σ is the instantaneous unbalanced water-vapor column. The group delay G is defined as

$$G \equiv \frac{\partial \phi}{\partial k} \tag{5}$$

which is easily found to be

$$G = x + N^w\Sigma + k\frac{\partial N^w}{\partial k}\Sigma \tag{6}$$

or, equivalently,

$$G = x + N^w\Sigma - \lambda\frac{\partial N^w}{\partial \lambda}\Sigma \tag{7}$$

One can derive an approximate value of G by replacing the derivative with a linearized approximation based on the refractivities in Table 1:

$$G \simeq x + N^w\Sigma - \lambda\frac{\Delta N^w}{\Delta \lambda}\Sigma \tag{8}$$

where ΔN^w and $\Delta\lambda$ are the changes in the respective quantities over a representative span of wavelength between λ_1 and λ_2, and λ and N are representative (e.g., average over wavelength) values.

The sum of the first two terms in the above expressions for G represent the overall phase delay. For a nondispersive system (i.e., one in which the third term vanishes) G is simply equal to the monochromatic phase delay $P = x + N^w\Sigma$. Thus it is natural to define a dispersion $D = P - G$ which has units of length and which vanishes when the dispersion does:

$$\begin{aligned} D &\equiv P - G \\ &= \lambda \frac{\partial N^w}{\partial \lambda} \Sigma \\ &= (\gamma^w)^{-1} \Sigma \end{aligned} \tag{9}$$

where for convenience we have defined the wavelength-dependent quantity

$$(\gamma^w)^{-1} \equiv \lambda \frac{\partial N^w}{\partial \lambda} \tag{10}$$

The quantity D is convenient to work with since both P and G are computed from the fringe quadratures and used internally by the interferometer servo system, independently of the effort to measure and correct for the effect of water vapor seeing. In the above expressions we have neglected the small dispersion due to the dry-air species; for a given choice of bandpass, the quantity D is essentially a tracer of the differential water column density Σ.

Plugging in the reference wavelengths above and setting $\Sigma = \sigma_\Sigma^{15}$ gives the RMS phase delay, group delay, and dispersion fluctuations in the two bands over a 15-minute period in median Mauna Kea conditions. The fluctuations in P are found to be 3.3 and 2.3 μm in the K band and the Nuller bandpass, respectively, and the corresponding fluctuations in G are 3.6 μm and 5.0 μm. The fluctuations in D are -0.33 μm and -2.6 μm, so we predict that the D fluctuations should be 7.8 times larger in the Nuller bandpass than in the K band. As we will see in the following sections, this prediction is borne out by the data.

It is worth noting here that the dispersion metric D has one subtle but important practical disadvantage: the phase delay P must be an *unwrapped* quantity, i.e., it runs monotonically over an arbitrarily large number of wavelengths. In the presence of strong dispersion it is nontrivial to define, let alone measure, this quantity in an absolute sense. Worse, it must be computed from time series of *wrapped* phase measurements and is thus vulnerable to unwrapping errors of some integer number of wavelengths. Such errors are often seen in practice when the star is faint or the seeing is poor. The practical impact of these limitations is that feedforward of information about the differential water column Σ must be AC-coupled, i.e., the absolute dispersion must ultimately be referenced to the measurements made by the Nuller itself, with the K-band fringe tracker providing only information about the short timescale water-induced fluctuations about that value.

Table 1. Refractivity per molecule of water vapor, computed from a sum over resonances, at wavelength λ.[3]

λ / μm	$k \times$ cm	Refractivity / cm^3
2.0	31419	9.092×10^{-24}
2.2	28560	9.029×10^{-24}
2.4	26180	8.926×10^{-24}
8.5	7392	7.756×10^{-24}
10.5	5984	6.491×10^{-24}
12.5	5027	5.035×10^{-24}

2.4. Feedforward of Phase and Group Delays

Given the above relationships between the water-induced phase delay P, group delay G, and the dispersion metric D, it is straightforward to compute the expected values in the Nuller bandpass from the measured values in the K band. Here we neglect the small dispersion due to the dry-air species, and the arbitrary offsets between the K band and Nuller values (i.e., we assume that the systems are AC-coupled). The differential water column is directly proportional to the dispersion metric as from the K-band data:

$$\Sigma = \gamma_K^w D_K \tag{11}$$

where $\gamma_K^w = -1.1 \times 10^{24}$ cm^{-3}. In general, this will not be a measurement of the absolute difference in the water column between the input beams, but will have an unknown (slowly varying) additional term due to dispersion in the instrument itself.

Given this column density and the phase delay in the K band it is easy to compute the phase and group delays in the Nuller bandpass, to within some unknown but slowly-varying offset:

$$P_{nuller} = P_K + (N_{nuller}^w - N_K^w)\ \Sigma \tag{12}$$

$$\begin{aligned} G_{nuller} &= G_K + (P_{nuller} - P_K) - (D_{nuller} - D_K) \\ &= G_K + [N_{nuller}^w - N_K^w - (\gamma_{nuller}^w)^{-1} + (\gamma_K^w)^{-1}]\ \Sigma \\ &= G_K + \psi\Sigma \end{aligned} \tag{13}$$

where for convenience we have defined

$$\psi = N_{nuller}^w - N_K^w - (\gamma_{nuller}^w)^{-1} + (\gamma_K^w)^{-1} \tag{14}$$

which depends only on the refractivity of water vapor at the relevant wavelengths. For the Keck Nuller the value of ψ is found to be 3.7×10^{-24} cm^3. The product $\sigma_{GD}^{15} = \sigma_\Sigma^{15}\psi$ is the 15-minute RMS fluctuation between the group delays measured in the K band and the Nuller bandpass. Its value is 1.4 μm.

3. KECK NULLER OBSERVATIONS OF TELLURIC WATER VAPOR

Simultaneous observations of water vapor seeing in the K band and the mid-infrared Nuller bandpass were made on UT 2005 October 19. The optical configuration was standard for the nuller, with the telescope pupils bisected by the Dual Star Modules (DSMs) so that fringes were formed simultaneously along two separate parallel 85 m baselines. The K-band light was separated from the mid-infrared light by dichroic mirrors, allowing simultaneous fringe monitoring in the two bands. Additional dichroic mirrors selected visible light for the AO wavefront sensors and for near-infrared J-band tip-tilt sensors (KATs) in the beam-combining lab.

The observations consisted of locking the adaptive optics systems of both Keck telescopes, and idling the K band fringe trackers (FATCATs[6]) and the Nuller fringe servos. The Fast Delay Lines (FDLs) dithered the OPD seen by each beam combiner by one wavelength, allowing the fringe phase delay and group delay to be monitored in each bandpass by examination of the fringe quadratures.[7] Only one long baseline was used in the mid-infrared for this test. The test was run for 5 minutes, which was long enough to sample most of the power in the water vapor differential column density fluctuations in typical Mauna Kea conditions.[5]

The target star was Epsilon Eridani ($m_V = 3.7; m_K = 1.7; F_\nu(N) = 9$ Jy; $\theta_{dia} = 2.1$ mas). The Nuller servo filter lengths were configured for "medium" sensitivity mode, which is typically useful for stars between ~ 10 and ~ 30 Jy in the N band. All internal and external metrology was active and helped to correct the rapid phase fluctuations due to internal vibrations by feeding forward the laser fringe position to the FDLs. No attempt was made to correct for the effects of water vapor seeing in realtime during the observations.

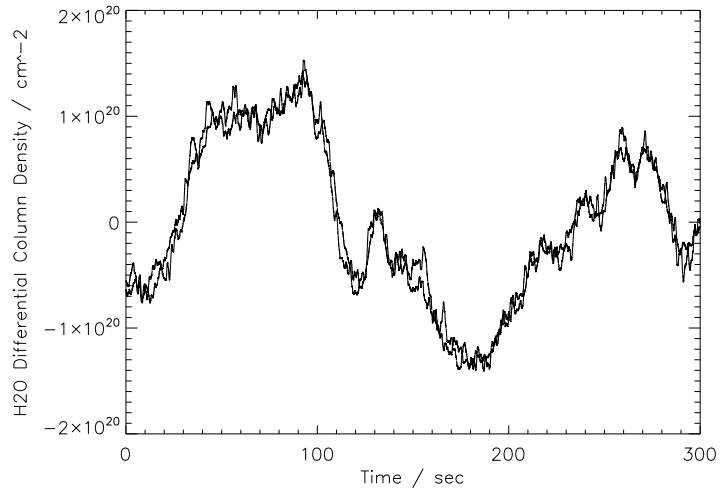

Figure 1. Water vapor differential column density Σ vs. time, measured in the K band in October 2005. These curves were derived from the dispersion metric D as described in Equation (11). They have been shifted to zero mean. The thick and thin curves are measurements from the "primary" and "secondary" long baselines, respectively; they trace each other with an RMS difference of 1.4×10^{19} cm^{-2}. Their correlation indicates that the water columns above the subapertures of the individual Keck telescopes are well correlated. The overall RMS fluctuation of the column density over the course of this 5-minute observation is 7.4×10^{19} cm^{-2}, which is twice as large as the σ_Σ^{15} value used in the calculations above even before correction for the different measurement times, indicating that this was a period of relatively strong water vapor seeing.

The realtime control (RTC) software produced estimates of the K-band phase and group delays at a 1 KHz rate. These values were smoothed with a 2-second boxcar filter to improve the SNR. The differential water column density Σ was computed as a function of time from the K-band data using Equation 11. It is plotted for both long baselines in Figure 1. The water seeing is found to be about twice as strong as in the median conditions.[5] The measurements along the two long baselines are essentially independent. The fluctuations are strongly correlated, giving confidence that the measurements are tracing a real atmospheric effect and confirming that the outer scale for water vapor seeing is larger than the ~ 5 m separation between the subapertures on one telescope. As expected from the power spectra measured in the radio, the most of the power in the fluctuations is in the lowest measured frequencies.

We next use the phase and group delays measured in the K band to compute their predicted values in the Nuller bandpass using Equations 12 and 13, and compare these predictions to the values measured directly by the Nuller. The results are plotted in Figures 2 and 3. The results are a bit surprising: while there are very clear correlations between the predicted and measured values, the errors in both quantities display a linear trend with essentially identical slope. The origin for this effect is not clear, but it appears likely to be produced by a slowly drifting optical component which is changing the OPD for the Nuller relative to that of the K-band fringe tracker.

Despite this anomaly, these results demonstrate that the refractivity of water vapor is behaving as theory says it should. This gives us confidence that measurements of its effects can be made in a bandpass where the SNR is high and transferred to one where the SNR is low, improving the overall performance of the instrument.

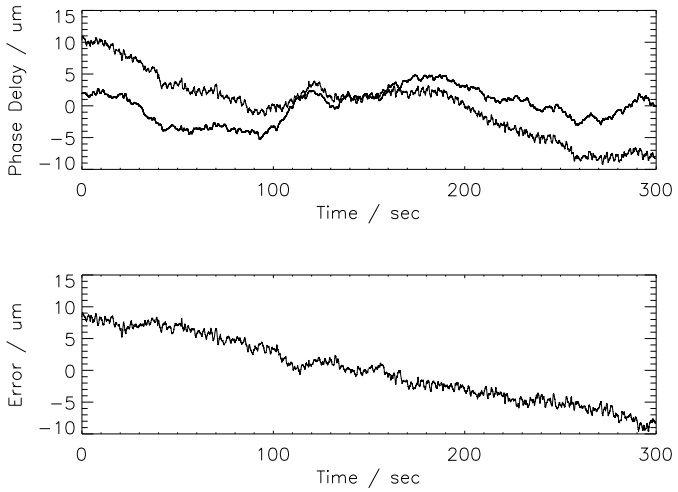

Figure 2. The top plot shows the phase delay measured in the Nuller bandpass (thick curve) and the prediction based on the K band measurement of the differential water column density in Figure 1 and Equation 12 (thick curve). They have been shifted to zero mean, as appropriate for an AC-coupled quantity. Their difference is shown in the bottom plot. The linear trend in the error was unexpected.

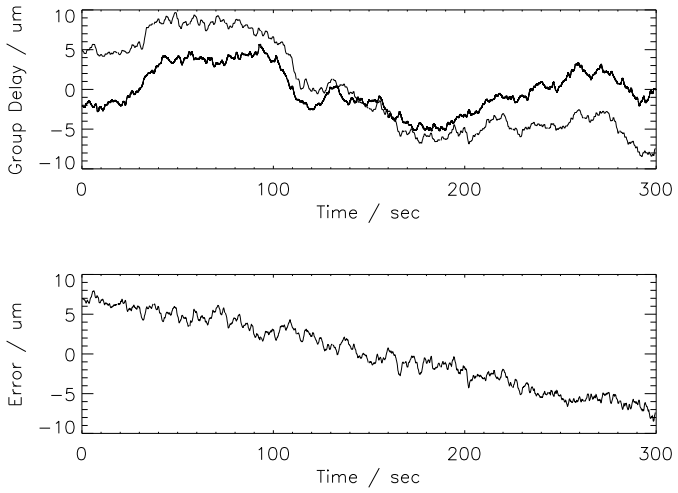

Figure 3. The top plot shows the group delay measured in the Nuller bandpass (thick curve) and the prediction based on the K band measurement of the differential water column density in Figure 1 and Equation 13 (think curve). They have been shifted to zero mean, as appropriate for an AC-coupled quantity. Their difference is shown in the bottom plot. The linear trend was unexpected and is not currently understood. Its similarity to the trend in the phase delay error suggests that there was a uniform change in the achromatic optical path difference of the Nuller relative to the K-band fringe tracker, perhaps because one of the optics was drifting.

ACKNOWLEDGMENTS

Funding was provided by NASA through the Keck Interferometer project. The W. M. Keck Observatory is operated as a scientific partnership among the California Institute of Technology, the University of California, and NASA. The Observatory was made possible by the generous Financial support of the W. M. Keck Foundation. The research presented here was conducted at the Jet Propulsion Laboratory, California Institute of Technology, and the Michelson Science Center, California Institute of Technology, under contract with the National Aeronautics and Space Administration. The authors wish to recognize and acknowledge the very significant cultural role and reverence that the summit of Mauna Kea has always had within the indigenous Hawaiian community. We are most fortunate to have the opportunity to conduct observations from this mountain.

REFERENCES

1. C.D. Koresko, M.M. Colavita, E. Serabyn, A. Booth, & J.I. Garcia "Measuring Extended Structure in Stars using the Keck Interferometer Nuller" *Proc SPIE* (these proceedings), 2006
2. C.D. Koresko, B.P. Mennesson, E. Serabyn, M.M. Colavita, R.L. Akeson, & M.R. Swain "Longitudinal dispersion control for the Keck interferometer nuller" *Proc. SPIE* **4838**, 625, 2003
3. M.M. Colavita, M.R. Swain, R.L. Akeson, C.D. Koresko, & R.J. Hill, "Effects of Atmospheric Water Vapor on Infrared Interferometry" *PASP* **116**, 876
4. L.S. Rothman, C.P. Rinsland, A. Goldman, S.T. Massie, D.P. Edwards, J.-M. Flaud, A. Perrin, C. Camy-Peyret, V. Dana, J.-Y. Mandin, J. Schroeder, A. McCann, R.R. Gamache, R.B. Wattson, K. Yoshino, K. Chance, K. Jucks, L.R. Brown, V. Nemtchinov, & P. Varanasi "The HITRAN Molecular Spectroscopic Database and HAWKS (HITRAN Atmospheric Workstation): 1996 Edition" *JQSRT* **60**, 665, 1998
5. C.R. Masson "Atmospheric effects and calibrations" *ASP Conference Series* **59**, 87, 1994
6. G. Vasisht, A.J. Booth, M.M. Colavita, R.L. Johnson, E.R. Ligon, J.D. Moore, & D.L. Palmer "Performance and verification of the Keck interferometer fringe detection and tracking system" *SPIE* **4838**, 824, 2003
7. M.M. Colavita "Fringe Visibility Estimators for the Palomar Testbed Interferometer" *PASP* **111**, 111, 1999